

Article

Microstructural Evaluation of Graphene-Reinforced Nickel Matrix Ni-P-Gr Coating on Ti-6Al-4V Alloy by the Electroless Coating Method

Hatice Gunduz ¹, Ramazan Karslioglu ^{2,3} and Fahrettin Ozturk ^{1,4,*}¹ Department of Mechanical Engineering, Ankara Yildirim Beyazit University, Ankara 06760, Turkey² Department of Industrial Design, Ankara Yildirim Beyazit University, Ankara 06760, Turkey³ AYBU Central Research Laboratory Research and Application Center, Ankara Yildirim Beyazit University, Ankara 06760, Turkey⁴ Turkish Aerospace Industries, Inc., Ankara 06980, Turkey

* Correspondence: fahrettin71@gmail.com or fahrettinozturk@aybu.edu.tr

Abstract: Titanium alloys are widely used in many industrial applications, from aerospace to automotive, and from defense to medical, as they combine superior properties such as high strength and low density. Still, titanium and its alloys are insufficient in environments with friction and wear because of their weak tribological properties. In the literature, numerous research works on improving the surface quality of titanium alloys have been conducted. Electroless coatings, on the other hand, are one of the most widely used surface improvement methods due to its homogeneous thickness achievement, high hardness, and good corrosion resistance. The autocatalytic reduction in the coating process enhances the surface quality of the material or alloy considerably. In addition, many studies in the literature aim to carry the properties of electroless coatings to a higher point by creating a composite coating with the addition of extra particles. In this study, graphene-reinforced nickel matrix Ni-P-Gr coating was applied to the surface of Ti-6Al-4V alloy, in order to enhance weak tribological behaviors, by the electroless coating method. Moreover, the coated and uncoated, heat-treated, and non-heat-treated specimens were subjected to abrasion in linear reciprocating ball-on-plate configuration to observe tribological properties. Microstructure examination of the samples was performed using a scanning Electron Microscope (SEM), X-ray Diffractometer (XRD), X-ray Photon Spectrometry (XPS), and Raman Spectroscopy. Specific wear rates of specimens were calculated using microstructural analysis and the hardness of the produced samples was measured using the Vickers hardness test. Results indicate that both the coating and the heat treatment improved the microstructure and tribological properties significantly. With the graphene-reinforced Ni-P coating via electroless coating process, the hardness of the substrate increased by about 34%, while it increased by approximately 73% using subjected heat treatment. Furthermore, the wear rate of the Ti-6Al-4V substrate was approximately 98% higher than that of the heat-treated nanocomposite coating. The highest wear resistance was obtained at the heat-treated nanocomposite coating.

Keywords: graphene; nanocomposite; nickel matrix coatings; titanium coating; electroless nickel coating; Ni-P electroless coating



Citation: Gunduz, H.; Karslioglu, R.; Ozturk, F. Microstructural Evaluation of Graphene-Reinforced Nickel Matrix Ni-P-Gr Coating on Ti-6Al-4V Alloy by the Electroless Coating Method. *Coatings* **2022**, *12*, 1827. <https://doi.org/10.3390/coatings12121827>

Academic Editor: Alicia de Andrés

Received: 10 October 2022

Accepted: 19 November 2022

Published: 25 November 2022

Publisher's Note: MDPI stays neutral with regard to jurisdictional claims in published maps and institutional affiliations.



Copyright: © 2022 by the authors. Licensee MDPI, Basel, Switzerland. This article is an open access article distributed under the terms and conditions of the Creative Commons Attribution (CC BY) license (<https://creativecommons.org/licenses/by/4.0/>).

1. Introduction

The surface properties of engineering materials directly affect the performance of applications because most of the failures such as corrosion, fatigue, wear, and friction occur on the material surface. Electroless Ni-P coating is widely used in many areas from the automotive to the computer industry since they have properties such as good corrosion resistance, high hardness, thickness uniformity, and good wear resistance [1,2]. Electroless Ni-P coating is an important surface improvement method to improve the

physical and chemical properties of materials due to the autocatalytic reduction process. Many researchers [3–7] have focused on the subject.

It has been stated in many studies in the literature that metal matrix composites are ahead of monolithic metals in terms of properties such as high strength, high electrical conductivity, high toughness, and low density [8–10]. In addition, it has been reported that metal matrix composite coatings can be produced by adding third-phase reinforcements to increase the properties of the coatings such as corrosion-wear resistance and strength, provided that they have biological and chemical compatibility [11–13].

It is common practice to obtain composite electroless nickel plating by adding various particles to electroless nickel plating [14–17]. These particles are completely and evenly distributed in the electroless nickel matrix and are firmly attached to the substrate, making electroless coatings more durable and long lasting than other lubrication and wear resistant alternatives [18]. It is widely accepted in the industry. In this application, it has been demonstrated that microhardness and tribological properties can be significantly improved by particle refining mechanism and charge transfer [19].

Carbon-based materials are the most common reinforcing materials used when creating electroless composite coatings. There have been several studies [20–30] in the literature characterizing their performance. Graphene nanoparticles, on the other hand, are one of the most advantageous carbon-based materials due to their ability to provide fracture strength up to 125 GPa and Young's modulus up to 1 TPa [31]. Thanks to its honeycomb-shaped hexagonal structure, graphene is endowed with numerous strengths such as being atomically thin, inert, wear-resistant, impermeable, and mechanically durable [23,32,33]. The addition of graphene-based materials to electroless nickel coatings has been a recent development and the properties of coatings has great attention. For example, Ni-P coatings prepared by Huihui et al. [20] with graphene oxide reinforcement showed excellent mechanical properties and hardness. Similarly, Tamilarasan et al. [21] synthesized Ni-P-GO with an electroless coating technique, and declared that graphene entering the Ni-P matrix could improve the wear properties of the coating alloy due to the lubricating effect of the graphene. Other researchers produced reduced graphene oxide (rGO) doped electroless Ni-P coating and revealed that the composite coating exhibits a rougher structure [22–24]. On the other hand, in other studies that produced metal matrix composite coatings using rGO, it was emphasized that the optimum amount of reinforcement should be adjusted, and it was revealed that adding a very high amount of rGO particles would adversely affect the hardness [25–27]. Hu et al. [28] used the electroless coating method for the first time for the synthesis of Ni/Graphene sheets and reported that no aggregates were formed despite obtaining a high nickel accumulation rate. Yu et al. [29] produced graphene-doped electroless Ni-P coatings on stainless steel specimens and reported that the graphene reinforcement gave higher Young's modulus and higher hardness.

On the other hand, in some studies in the literature, Ni-P coating and Ni-P-Gr coatings were studied together. The effects of graphene on Ni-P coating were investigated. Mindivan et al. [32] used St-37 substrate in their studies where they produced Ni-P and graphene nano-plate-reinforced Ni-P coating by electrolytic coating method. They found that the lowest wear rate and the highest hardness would be obtained in the composite coating. As a result of microstructural investigations, they stated that this improvement was due to the more compact structure of the composite coating. Uysal [26] produced Ni-P coatings using electroless coating method in his study using mild steel as a substrate. They investigated the effects of graphene oxide and TiO₂ particles on morphology, corrosion and tribological properties, and as a result, they revealed that the presence of graphene oxide and TiO₂ particles improved the hardness of the coating. Yu et al. [29] prepared pure Ni-P coating and graphene-reinforced Ni-P coatings by ultrasonic-assisted electroless plating on mold material (06Cr25Ni20) substrates. In this study, which aims to improve the mechanical properties, the hardness value of the Ni-P coating increased from 1096.4 to 1184.6 HV, while the Young's modulus of the composite coating increased by 8.2%. In other studies using different substrates, it was reported that graphene reinforcement improves

the properties of the Ni-P coating, and the composite coating is particularly tribologically advanced compared to the pure Ni-P coating [23,25,28].

Titanium and its alloys have excellent mechanical and physical properties such as high strength, low weight, and remarkable corrosion resistance, so it is used in many industries, especially in aerospace. Especially, Ti-6Al-4V is a light but strong alloy and saves weight in highly loaded structures, so it is extremely suitable for jet engines, gas turbines, and many airframe components [34–37]. Although titanium and its alloys have been widely used in many areas due to its advanced physical and mechanical properties, unfortunately, it is insufficient in areas which require wear and friction resistance due to electron arrangements and crystalline structures. Many surface improvement methods have been tested to improve the tribological properties of titanium and its alloys [38–41].

The purpose of this study was to investigate the effects of electroless Ni-P coating with graphene nanoparticle reinforcement on the microstructure and weak tribological properties of Ti-6Al-4V. Ni-P-Gr coatings have been produced on different types of substrates by an electroless-deposition method in many studies in the literature. However, to the best of our knowledge, there have been no studies on the production of Ni-P-Gr film, which is associated with the tribological properties of Ti-6Al-4V by electroless deposition method. In addition, the effect of heat treatment on microstructure and tribological properties of the uncoated and coated titanium alloys was investigated. It was found that graphene-reinforced Ni-P matrix nanocomposite coating could be successfully applied on Ti-6Al-4V substrate. Microstructural properties of heat-treated and non-heat-treated, non-coated, and nanocomposite layers were investigated by Scanning Electron Microscopy (SEM), X-ray Diffractometer (XRD), X-ray Photon Spectrometry (XPS), and Raman Spectroscopy. In addition, tribological and mechanical properties were analyzed by a reciprocating the ball-on-plate and the Vickers microhardness test devices. It was concluded that graphene addition and heat treatment remarkably improved the microstructure and tribological properties.

2. Materials and Methods

In this study, Ti-6Al-4V titanium substrates were used. All the substrates have 50 mm × 50 mm × 2 mm dimensions at the beginning of the processes. Surface preparation processes were applied to the Ti-6Al-4V substrates before the coating process. Due to their thermodynamic behavior, titanium alloys tend to form a passive and persistent oxide layer, making it difficult to coat. In addition, if electroless nickel coatings are applied to dirty or oxidized surfaces, desired coating quality cannot be achieved. In order to prevent the oxidation of the titanium surface, the zincating process was carried out. The surface preparation, activation, and oxide layer avoidance processes applied for the Ti-6Al-4V substrates in order. The substrates were degreased with acetone and then air-dried. Afterward, the chemical etching process of the substrates immersed in a 6% hydrogen fluoride (HF) acid solution was completed and rinsed in deionized water. Afterward, the samples, which were zincate for 90 s and then dipped directly into the nanocomposite coating solution. Commercial electroless Ni-P coating solution was used for the coating process. A total of 2 g/L graphene nanoparticle was added to the solution. The average radius of the graphene nanoparticle is 1.5 μm. Electroless nickel phosphate graphene coating bath was mixed with an ultrasonic homogenizer for 1 h in order to prevent the nano powders from clumping and collapsing during the coating process. The coating process took 60 min, the temperature was kept at 90–92 °C during the process and a magnetic stirrer was used to ensure homogeneous mixing. It is a well-known fact that the superiority of the Ni-P-Gr composite coating over the Ni-P coating has already been proven. Therefore, pure Ni-P coating was not applied and eventually a comparison was not made.

In order to observe the effect of the heat treatment after the coating process, a group of samples were exposed to heat treatment. After the electroless coating process was performed, samples were separated into two groups and one was heat-treated for 1 h at 450 °C in an argon atmosphere heat treatment furnace and then the samples were left to

cool down for all night long. The other group was left as non-heat-treated. The wear and friction tests of the samples were carried out in the linear (reciprocating) module of the UTS Tribometer T30M-HT (UTS Scientific Instruments, Trabzon, Turkey) wear test device. The wear tests are based on the ball-on-plate tribo-testing configuration technique and the schematic view of reciprocating wear mechanism is shown in Figure 1. The experiments were carried out at room temperature (RT), in an oil-free environment, under a normal load of 1 N. A ball made of Al_2O_3 with a diameter of 10 mm was used to wear samples with a constant sliding speed of 100 mm/s for the total sliding distance of 100 m.

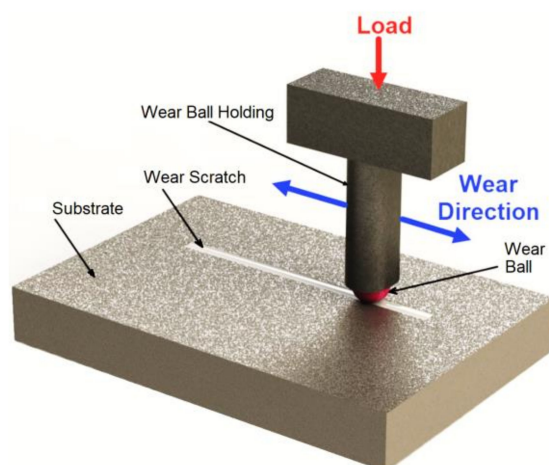


Figure 1. Schematic view of reciprocating wear mechanism.

Surface morphologies were analyzed by Scanning Electron Microscope (Hitachi SU5000, Tokyo, Japan) and Raman analyses were performed with Jasco NRS-4500 Raman spectrometer (Easton, MD, USA) in Ankara Yıldırım Beyazıt University (AYBU) Central Laboratory. The elemental analysis was performed using a PANalytica X'pert Pro MDP Brand XRD scanning device (Great Neck, NY, USA) with Cu K alpha monochromator at a speed of $2^\circ/\text{min}$. The wavelength of the beam is 1.54059 \AA . The analysis of the peaks from the XRD analysis was conducted with the help of computer software. The crystal structure characterization of the Ni-P-Gr coating layer produced in the study, the region where 2θ is between 10° and 110° , was investigated. The chemical composition was investigated by XPS analysis. In addition, XPS measurements were performed on the PHI 5000 Thermo Scientific K-Alpha instrument (Waltham, MA, USA) with a 50 W X-ray anode sourced from monochromatic Al-K (1486.6 eV) beams at a vacuum of 10^{-10} Torr. X-ray Photoelectron Spectroscopy (XPS) analyzes were taken on both the normal sample surface and wear marks. Before starting the analysis, ion beam etching was conducted. This process was performed in order to clean the surface, in case there was 10 nm of pollution, oxidation, etc. on this surface. While looking for nickel, carbon, phosphate, and oxygen in the analysis of normal surfaces, aluminum was also added to the analysis of the wear marks, being the material of the ball. Vickers microhardness studies were carried out for the nano composite coatings, and a load of 200 gr was applied for 15 s in the measurements made using the Matsuzawa HWMMT-X3 brand microhardness test device (Tokyo, Japan). In this study, the microstructural examination of the composite coating was carried out using SEM images, while the presence of graphene was investigated using the XPS and the Raman spectrum analyses. For this reason, the measurement of the coating thickness of the samples was measured using a Leica CTR6000 microscope (Wetzlar, Germany).

3. Results and Discussion

The sectional images taken using a microscope are displayed in Figure 2a,b for the titanium alloy substrate and the nanocomposite coating, respectively. In Figure 2b, the substrate, the substrate-coating interface, and the coating are clearly visible. The interface

lies homogeneously on the substrate. Different studies have stated that, since the electroless coating process takes place in the bath solution, the homogeneous coating thickness was obtained regardless of the substrate shape, and Figure 2b supports this information [42–45]. Also, with the use of the microscope's own scale, ten different measurements were taken on the coating. These measurements yielded a mean coating thickness of 12.47 μm . In a study by Meshram et al. [46], Ni-P and Ni-P-Gr coatings were successfully deposited on the substrate via the electrodeposition method for 1 h. As a result, the coating thickness for Ni-P coating was approximately 3.30 μm , while the coating thickness was found to be approximately 7 μm for each ratio with graphene reinforcement at different ratios. Graphene added to the Ni-P matrix provides more surface area for the reduction in nickel-phosphorus, which may increase the deposition rate leading to the observed increase in the thickness of the graphene-reinforced coatings [46]. Although the coating time of this study is the same, the reason for obtaining a higher coating thickness than that in the Meshram's study can be explained by the addition of graphene at a higher rate. As a matter of fact, the volume of graphene entering the structure increases due to the increase in the graphene added to the bath composition by weight [47]. Likewise, Yasin et al. [47] aimed to produce graphene-reinforced Ni-P coating at different rates using the electrochemical coating technique in their study and obtained the maximum coating thickness at the maximum graphene ratio (0.4 g/L).

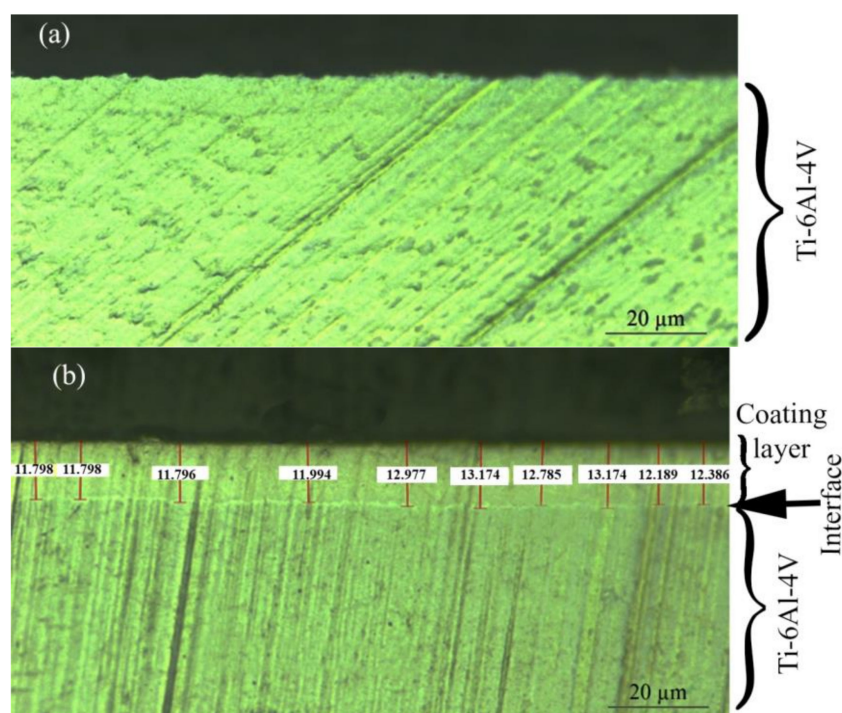


Figure 2. Section from (a) Ti-6Al-4V, (b) coated sample.

After the successful coating operations, the surfaces were investigated. Figure 3 shows SEM and EDS images of the graphene-doped nickel matrix nanocomposite of Ti6-Al-4V alloys. When the surface morphology of the Ti-6Al-4V alloy was examined, it was clearly seen that there were surface segregations. These segregations were caused by the coaxial α phase and the intergranular β phase in the Ti-6Al-4V alloy microstructure [48]. In the EDS elemental analysis, the elements on the surface of the Ti-6Al-4V alloy are as shown in Figure 3b; after the coating process was applied to the substrate, both the surface morphology and the elemental composition were completely changed and this change is shown in Figure 3c,d, respectively. A homogeneous, crack-free, non-porous, and spherical microstructure was obtained with the coating process. In many studies in the literature, it was pointed out that this nodular microstructure is the characteristic feature of nickel

phosphate coating [49]. On the other hand, when the elemental analysis of the coating is examined, as shown in Figure 3d, it can be understood that the elements belong to the coating on the surface instead of the Ti-6Al-4V alloy. These results prove that the composite coating layers were successfully deposited on the substrate.

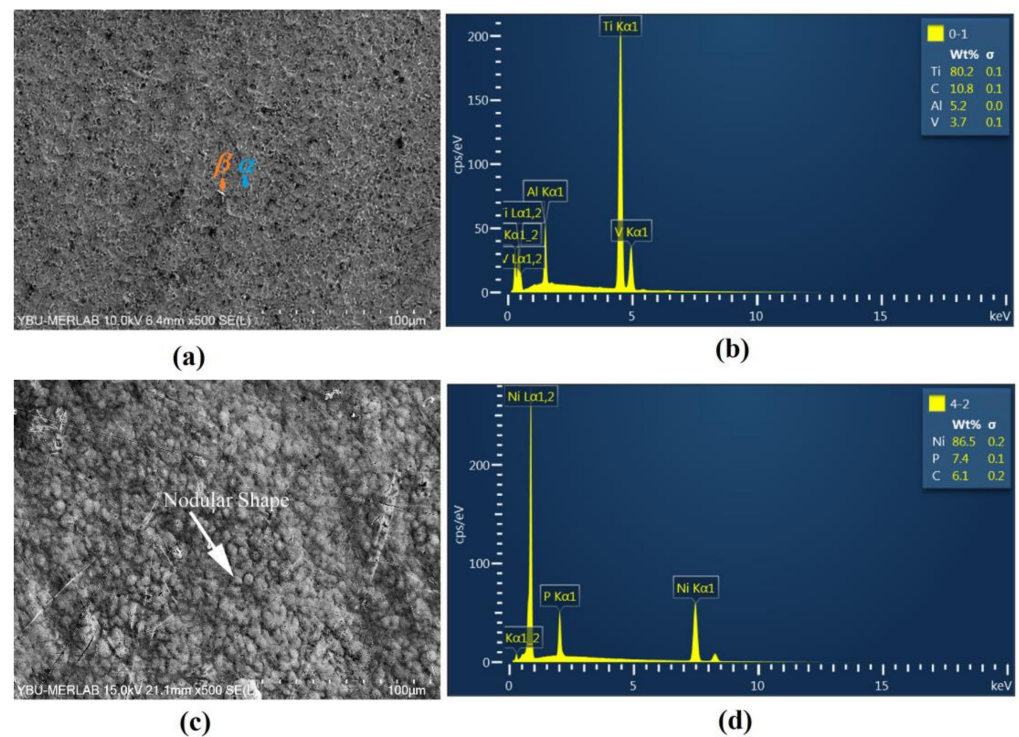


Figure 3. Surface morphologies and SEM, EDS images of the substrates (a) SEM image of Ti-6Al-4V; (b) EDS image of Ti-6Al-4V; (c) SEM image of Ni-P-Gr; (d) EDS image of Ni-P-Gr.

As shown in Figure 4, the effects of both the coating and heat treatment on the crystal structure of the samples were investigated by the XRD. Figure 4a shows the crystal structure of Ti-6Al-4V, while Figure 4b belongs to the Ni-P-Gr composite coating. The blue lines in the figures are for the samples that are not heat-treated and the orange lines are for the samples that are heat-treated. Evans et al. [50] stated that crystallinity decreased at the XRD profiles where wide, low, and smooth domes replaced with sharp peaks. The crystalline structure shown with the blue line in Figure 4a undergoes a change and an amorphous structure occurs due to the coating process. This transformation is an expected change since it is known from the research in the literature that the micro structure of the Ni-P coating is also amorphous [51–53]. On the other hand, the blue line indicates the amorphous structure in Figure 4b which is transformed a crystalline structure by heat treatment indicated by the orange line. Amorphous materials are metastable and become stable by heat treatment [18]. A careful examination of the XRD of the Ni-P-Gr coating shows that there is a large peak of face-centered cubic (FCC) Ni (111) at the point where the amorphous and crystalline structures coexist and 2θ equals 45° .

Figure 5 demonstrates the average Vickers hardness values. The highest hardness value was measured at the heat-treated nanocomposite coating. An increase in the microhardness value was observed due to the coating process. It is based on the grain size reduction which generates the crystalline strengthening mechanism and also graphene can avoid dislocation movement in the nickel matrix [32,54–58]. The heat treatment significantly changes the hardness of the Ni-P coating [3,43,59]. As a matter of fact, while the average hardness of the nanocomposite coating was 438.52 HV, it increased by approximately 29% during the heat treatment and became 566.9 HV.

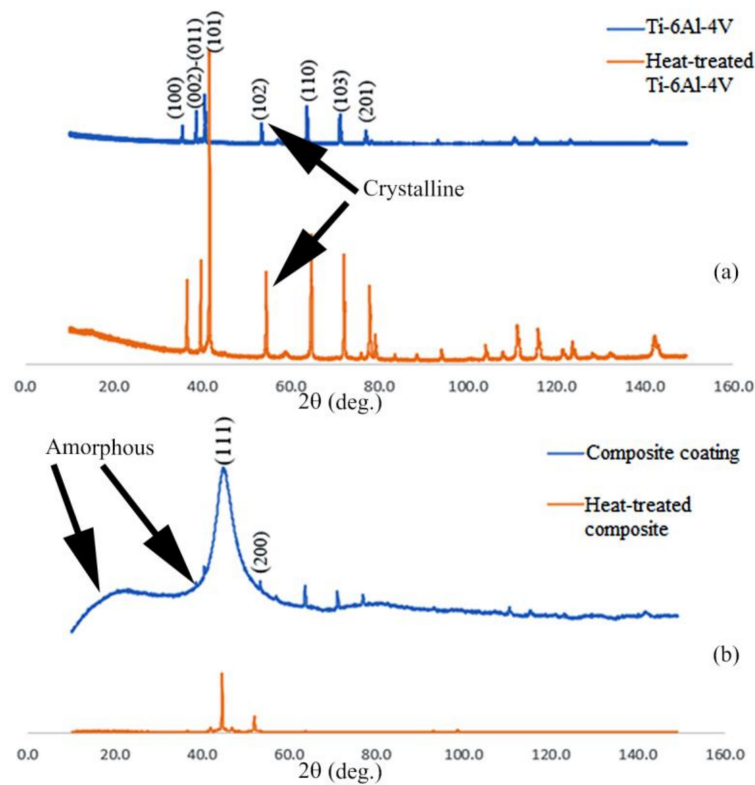


Figure 4. XRD patterns of (a) Ti-6Al-4V and (b) the coated sample, the blue lines show the non-heat-treated samples, while the oranges are for the heat-treated samples.

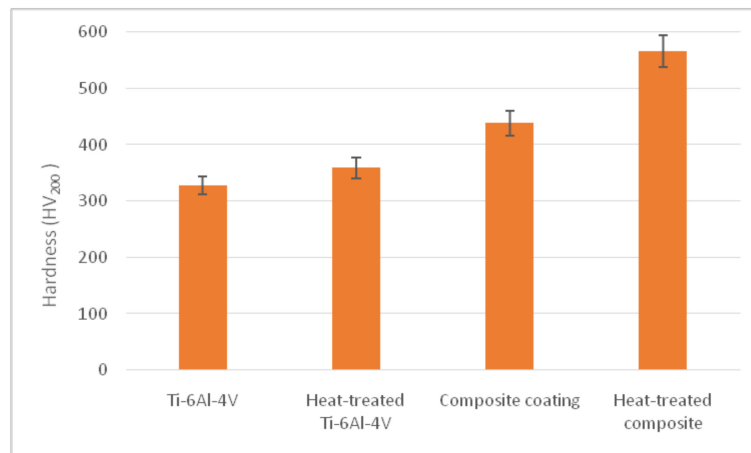


Figure 5. Average micro hardness values.

After the linear reciprocating wear process, wear traces were formed, and the high magnification of SEM photographs of these wear traces are shown in Figure 6. The red arrow in the figure indicates the sliding direction of the abrasive ball. Figure 6a, b are images of untreated and heat-treated Ti-6Al-4V substrates, respectively. During the linear reciprocating motion of the abrasive ball, slip lines parallel to the ball movement were formed due to the plastic deformation on both surfaces. Based on the studies in the literature, this can be interpreted as the occurrence of abrasive wear [58,60,61]. In Figure 6a, partial eruptions are also visible on the worn surface of the samples that are non-heat-treated. Since Xu et al. [59] stated that the adhesive wear mechanism could be seen as eruptions in SEM images. These eruptions are associated with the predominant wear

mechanism being the adhesive wear mechanism. In Figure 6b, however, the dominant wear mechanism underwent abrasive wear, as the debris resulting from this adhesive wear decreased.

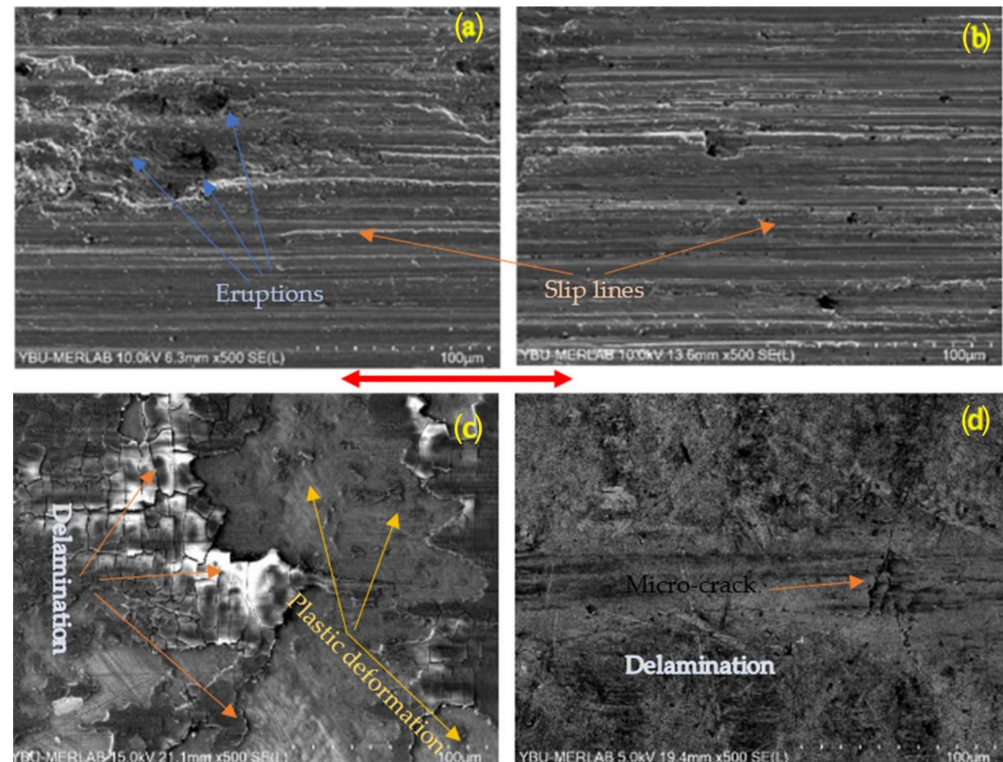


Figure 6. Wear traces of substrates: (a) non-heat-treated and (b) heat-treated Ti-6Al-4V; (c) non-heat-treated and (d) heat-treated Ni-P-Gr.

Figure 6c,d shows SEM images of non-heat-treated and heat-treated Ni-P-Gr nanocomposite coatings, respectively. As can be seen from the microstructure in Figure 6c, plastic deformation occurred because of the abrasive forces acting on the substrate, and microcracks turned into debris. Similar wear mechanism has been observed in studies in the literature and this wear mechanism has been associated with delamination. [26,32,60,62]. In addition to this, the presence of abrasive wear traces is also seen in the samples that are non-heat-treated. On the other hand, when the microstructure of the heat-treated coating was examined, it was observed that microcracks formed due to the loads on the substrate during the wear tests, but these cracks did not progress enough to cause delamination. When considered together with the hardness results presented above, the failure of the cracks to progress and the minimum amount of wear can be associated with the highest hardness in this sample. As a matter of fact, it is the subject of many studies that hardness and wear resistance are directly proportional [63–65]. When the figures are examined, it can be seen that the most wear traces are observed in Ti-6Al-4V samples, and as a result of the heat treating and coating, partial spills occur in the Ti-6Al-4V heat-treated sample, while only micro-cracks occur in the heat-treated coating. Abrasive wear resistance decreases with increasing hardness, which proves the change in the dominant wear mechanism in the composite coating. When the hardness increases, abrasive wear resistance decreases; therefore, regarding the change of the dominant wear mechanism, it can be proven that the hardness increases regarding both the heat treatment and coating [61].

On the other hand, the wear scar widths formed after the wear tests are shown in Figure 7. Trace widths were measured using the ImageJ software program and found to be 1.226 mm for Ti-6Al-4V (Figure 7a). The effect of heat treatment on the wear scar width is seen in Figure 7b and the scar width with heat treatment decreased slightly to

1.127 mm. Moreover, the wear scar width was measured as 0.367 mm for the Ni-P-Gr nano composite coating and 0.342 mm for the heat-treated coating. This reduction in track width can be interpreted as the composite coating, significantly increasing the wear resistance of the surface. As a matter of fact, it has been mentioned in many studies in the literature that the Ni-P-Gr coating improves the tribological properties of different surfaces. Mindivan et al. [32] and Algul et al. [58] produced graphene-reinforced Ni-P coatings by electroplating and found that the wear marks on the composite coated surface were reduced. The main reason is the fact that the composite coating increases the hardness and graphene has solid lubricating properties [66].

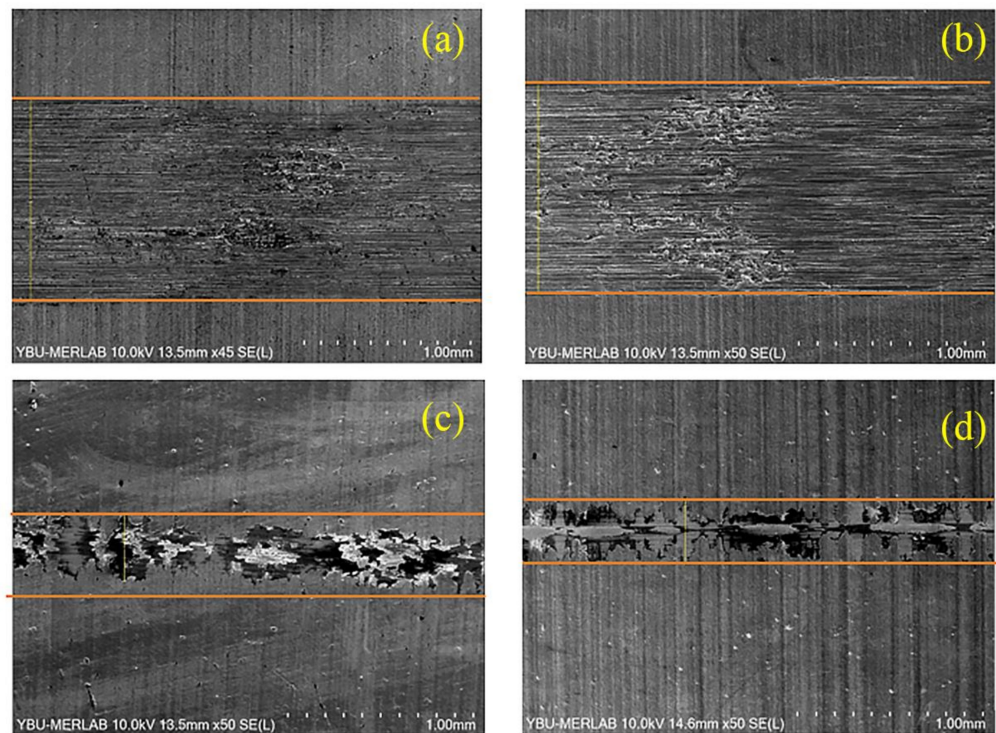


Figure 7. SEM morphologies of the wear tracks of substrates: (a) Ti-6Al-4V (b) Heat-treated Ti-6Al-4V (c) Composite coating (d) Heat-treated composite coating. The orange lines show the wear mark width and the yellow lines are the parallel lengths calculated by the ImageJ program.

The volume of wear loss was calculated geometrically using the wear scar width data measured with ImageJ V 1.8.0 software in Figure 7a–d. The calculated wear scar geometry is presented in Figure 8. Then, the specific wear rate was calculated using Equation (1) [67],

$$Wr = W/NL \quad (1)$$

where Wr is the specific wear rate [$\text{mm}^3/(\text{Nm})$], N is the normal load, L is the sliding distance, and W is the calculated wear volume [67]. Specific wear rates were calculated as shown in Figure 9. The wear rate decreased significantly with the electroless coating process, this rate increased even more with the effect of the heat treatment, the lowest specific wear rate was obtained in the heat-treated coating. The calculated wear rates were 8.22, 6.38, 0.24 and $0.19 (\times 10^{-9}) \text{ mm}^3/\text{Nm}$, respectively. The specific wear rate for Ti-6Al-4V reduced by approximately 22% due to the effect of heat treatment. The wear rate was reduced by approximately 98% by the graphene enhanced nickel-phosphorus coating of Ti-6Al-4V. In addition, the heat treatment negatively affected the wear rate of the coated sample, and a 21% reduction was achieved in the wear rate. As a result, it has been observed that both the heat treatment and the composite coating increase the wear resistance of the Ti-6Al-4V material. The highest wear resistance was observed in the

heat-treated Ni-P-Gr nanocomposite coating. In other studies in the literature, it has been emphasized that the wear resistance increases, especially with graphene reinforcement [62]. During the tribological test, the temperature rises at the contact surface due to frictions. Graphene is not stable at high temperatures; therefore, graphene converts to graphite on nanocomposite surfaces. The converted graphites significantly reduce the coefficient of friction due to the high temperature generated on the friction surfaces, another factor that reduces wear loss [68].

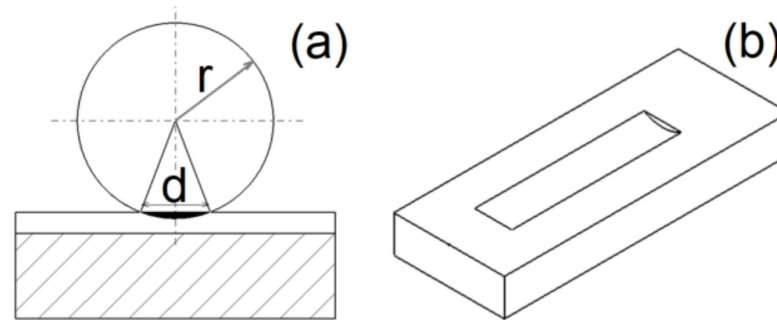


Figure 8. The wear scar generated by reciprocating sliding motion of the ball on a flat specimen; (a) 2D view of the wear scar [67] (b) 3D view of the wear scar [62].

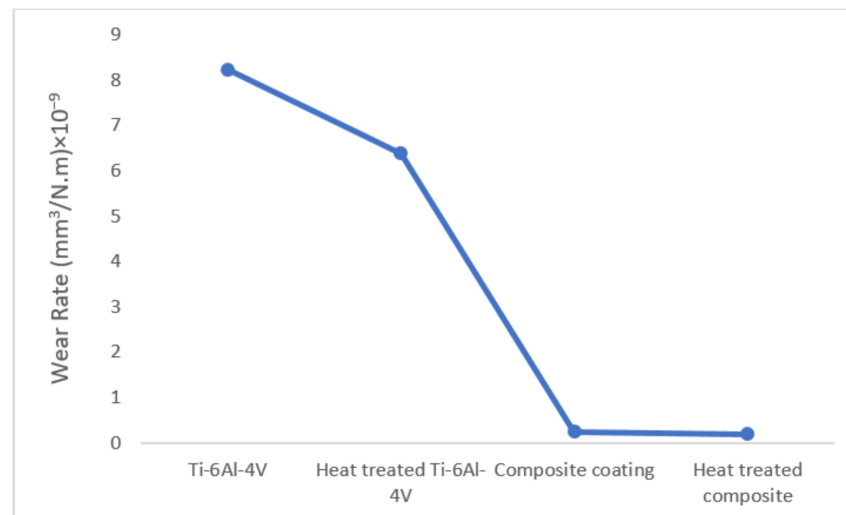


Figure 9. Specific wear rates.

The chemical composition of the Ni-P-Gr composite coating was investigated using the XPS analysis and the spectra obtained from the coating surface are given in Figure 10a–d. The Ni2P spectrum of the Ni-P-Gr composite coating was characterized by a highly intensity peak at 853.3 eV. This spectrum could be related to the nickel element [69,70]. Moreover, graphene's chemical state is sp² and the binding energy for this state is approximately 284 eV [71]. A C1s peak was observed on approximately 284 eV in Figure 10a,b. In Figure 10c,d, an Ni2P spectrum was observed about 854 eV. These peaks indicate the presence of nickel and graphene in chemical composition.

Raman spectroscopy plays an important role in the structural characterization of graphene-based materials, and Figure 11a–d show the Raman spectroscopy of the non-heat-treated and heat-treated composite coatings. Raman spectroscopy provides important information about graphene defects and stacking. Graphene can be clearly distinguished from graphite by the Raman spectrometry [72]. The main features in the graphite/graphene Raman spectrum are represented by the D, G, and 2D peaks. A G peak at approximately 1580 cm^{-1} and a 2D peak at approximately 2700 cm^{-1} is observed on graphite samples.

It was seen that the 2D graphite tape always has a shoulder of about 2650 cm^{-1} and this shoulder represents graphite. The D band was found at about 1330 cm^{-1} and is indicative of defects in the sample [1,73,74]. As seen in the figure, each sample has a D peak at approximately 1370 cm^{-1} , a G peak at 1590 cm^{-1} , and a 2D peak at 2790 cm^{-1} , and there was no shoulder on the 2D peak in any of the samples. The Raman spectra obtained from composite coatings confirm that graphene was successfully reinforced into nickel-phosphorus obtained by the electroless coating method. In Figure 11a,b, the peak densities decreased a little bit with the effect of heat treatment, and in Figure 11c, it underwent a great change with the effects of wear and heat treatment. In Figure 11d, the peak intensities have approached zero. After searching the literature, we found that it has been concluded that structural defects occur in graphene structures due to the mechanical loads occurring during wear and the high-temperature effect caused by friction, and due to these defects, the graphene structure deteriorates and transforms into a graphite-like structure [61]. Graphite is known to be one of the most widely used lubricants. In this case, when the wear and the Raman analysis results were examined together, it was determined that these graphite-like structures reduce the wear loss at the interface.

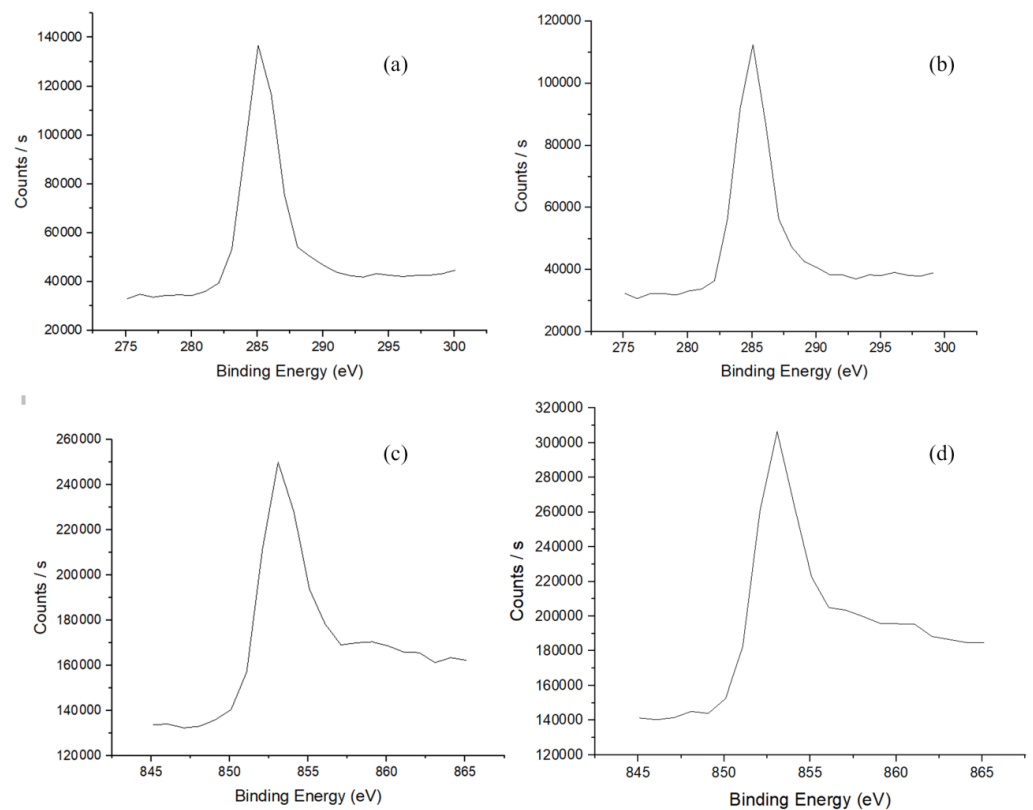


Figure 10. C1s and Ni 2p_{3/2} regions of high-resolution XPS spectra obtained with carbon and Ni in the Ni-graphene nanocomposite coating: (a) C1s on surface; (b) C1s on scratch; (c) Ni2P on surface; (d) Ni2P on scratch.

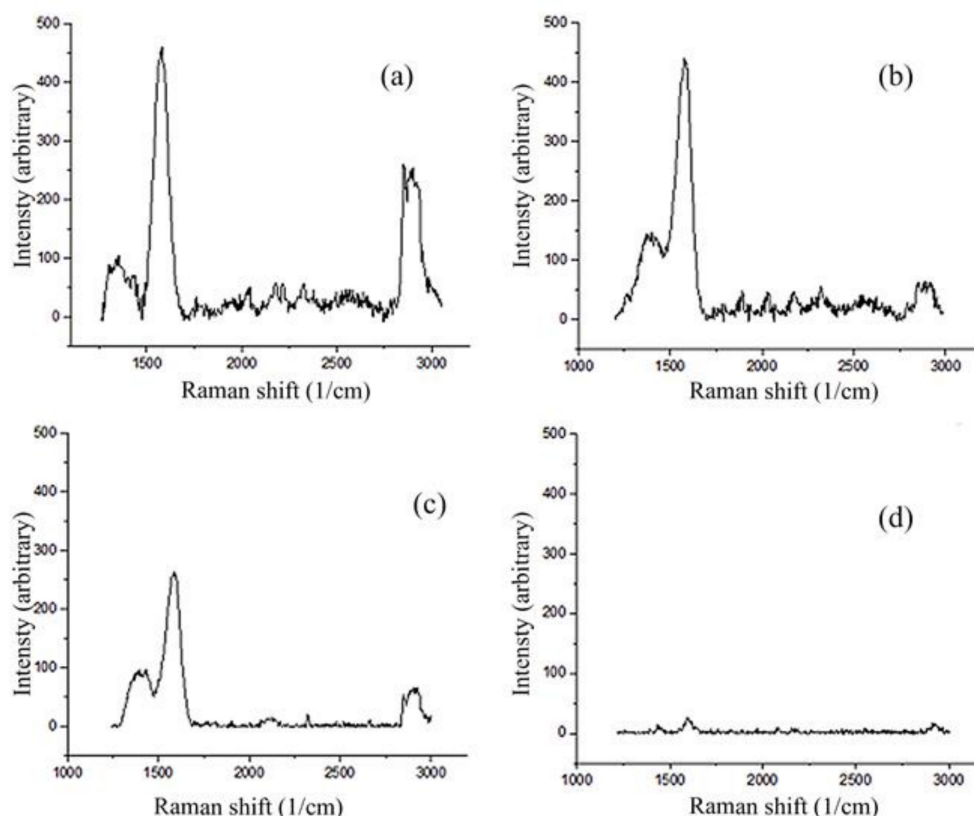


Figure 11. Raman spectroscopy of composite coating: (a) coated surface; (b) coated scratch; (c) coated heat-treated surface; (d) coated heat-treated scratch.

4. Conclusions

In this study, graphene-reinforced nickel matrix Ni-P-Gr coating was applied to the surface of Ti-6Al-4V alloy using the electroless coating method. The effects of composite coating and heat treatment on microstructure and tribological properties were investigated. Following conclusions were drawn:

- The Gr-Ni-P coating was successful. The microstructure of titanium alloy turned into a nodular structure. In addition, a 12.47 μm coating thickness was achieved on titanium alloy substrates.
- The crystal structure of the Ti-6Al-4V material turned into an amorphous structure with the composite coating process.
- The heat treatment applied to the composite coating caused the phase transformation and made the crystal structure more stable.
- The heat treatment had a positive effect on the wear resistance in both coated and uncoated structures.
- Both coating and heat treatment had a positive effect on the microhardness values. The highest hardness value of 566.9 HV was achieved at the heat-treated Ni-P-Gr coating.
- It was observed that the wear was higher in uncoated samples. The lowest wear scar width was obtained in the heat-treated graphene-reinforced nanocomposite coating.
- The highest wear resistance was obtained in the heat-treated nanocomposite coating.
- In the XPS analysis, binding energies of approximately 284 and 853 eV were obtained, revealing the presence of Gr and Ni in the coating structure, respectively.
- Raman spectrometry analysis revealed that the lubrication property was increased with the heat treatment.
- The wear rate of the Ti-6Al-4V substrate is approximately 98% higher than that of the heat-treated nanocomposite coating. The highest wear resistance was observed on the heat-treated nanocomposite coating.

Author Contributions: Conceptualization, R.K.; Methodology, R.K. and H.G.; Validation, experimental study and characterization, H.G., Supervision, R.K. and F.O.; Writing—original draft, H.G.; Writing—review & editing, F.O. All authors have read and agreed to the published version of the manuscript.

Funding: This study was supported by Ankara Yildirim Beyazit University (AYBU), Scientific Research Projects Unit (FYL-2021-2229).

Institutional Review Board Statement: Not applicable.

Informed Consent Statement: Not applicable.

Data Availability Statement: Not applicable.

Acknowledgments: AYBU support is greatly appreciated.

Conflicts of Interest: The authors declare no conflict of interest.

References

1. Su, F.; Liu, C.; Guo, J.; Huang, P. Characterizations of nanocrystalline Co and Co/MWCNT coatings produced by different electrodeposition techniques. *Surf. Coat. Technol.* **2013**, *217*, 94–104. [\[CrossRef\]](#)
2. Mina, M.; Bastwros, H.; Esawi AM, K.; Wifi, A. Friction and wear behavior of Al-CNT composites. *Wear* **2013**, *307*, 164–173.
3. Mallory, G.O.; Hadju, J.B. *Electroless Plating: Fundamentals and Applications*; American Electroplaters and Surface Finishers Society: New York, NY, USA, 1990.
4. Zhang, Q.; Wu, M.; Zhao, W. Electroless nickel plating on hollow glass microspheres. *Surf. Coat. Technol.* **2005**, *192*, 213–219. [\[CrossRef\]](#)
5. Martyak, N.; McCaskie, J. Speciation in electroless nickel solutions. *Plat. Surf. Finish.* **1996**, *83*, 62–66.
6. Wang, X.C.; Cai, W.B.; Wang, W.J.; Liu, H.T.; Yu, Z.Z. Effects of ligands on electroless Ni-P alloy plating from alkaline citrate-ammonia solution. *Surf. Coat. Technol.* **2003**, *168*, 300–306. [\[CrossRef\]](#)
7. Pei, S.; Li, S.; Zhong, L.; Cui, K.; Yang, J.; Yang, Z. Analysis of the causes of differences between the upper and lower surfaces of electroless Ni-P Coating on LZ91 Magnesium-Lithium Alloy. *Coatings* **2022**, *12*, 1157. [\[CrossRef\]](#)
8. Mazumdar, S.K. *Composites Manufacturing: Materials, Product and Process Engineering*; CRC Press LLC: Boca Raton, FL, USA, 2002.
9. Akbulut, H. Alümina Fiber Takviyeli Al-Si Metal Matriksli Kompozit Üretimi ve Mikroyapı Özellik İlişkilerinin İncelenmesi. Ph.D. Thesis, İstanbul Teknik Üniversitesi, İstanbul, Turkey, 1995.
10. Evans, A.; SanMarchi, C.; Mortensen, A. *Metal Matrix Composites in Industry: An Introduction and a Survey*; Chawla, N., Chawla, K.K., Eds.; Metal Matrix Composites; Springer: New York, NY, USA, 2003.
11. Bakhita, B.; Akbaria, A.; Nasirpouria, F.; Hosseini, M.G. Corrosion resistance of Ni-Co alloy and Ni-Co/SiC nanocomposite coatings electrodeposited by sediment codeposition technique. *Appl. Surf. Sci.* **2014**, *307*, 351–359. [\[CrossRef\]](#)
12. Gül, H.; Kılıç, F.; Uysal, M.; Aslan, S.; Alp, A.; Akbulut, H. Effect of Particle Concentration On the Structure and Tribological Properties of Submicron Particle Sic Reinforced Ni Metal Matrix Composite (MMC) Coatings Produced by Electrodeposition. *Appl. Surf. Sci.* **2012**, *258*, 4260–4267. [\[CrossRef\]](#)
13. Gül, H.; Akbulut, H.; Aslan, S.; Alp, A. Effect of Reciprocating Sliding Speed on the Tribological Performance of Nano SiCp Reinforced Ni-Metal Matrix Composites Produced by Electrocodeposition. *J. Nanosci. Nanotechnol.* **2012**, *12*, 9076–9087. [\[CrossRef\]](#)
14. Ding, X.; Wang, W.; Zhang, A.; Zhang, L.; Yu, D. Efficient Visible Light Degradation of Dyes in Wastewater by Nickel-phosphorus Plating-titanium Dioxide Complex Electroless Plating Fabric. *J. Mater. Res.* **2019**, *34*, 999–1010. [\[CrossRef\]](#)
15. Hsu, C.-I.; Hou, K.-H.; Ger, M.-D.; Wang, G.-L. The Effect of Incorporated Self-Lubricated BN(h) Particles on the Tribological Properties of Ni-P/BN(h) Composite Coatings. *Appl. Surf. Sci.* **2015**, *357*, 1727–1735. [\[CrossRef\]](#)
16. Huang, Z.; Zhou, Y.; Nguyen, T. Study of nickel matrix composite coatings deposited from electroless plating bath loaded with TiB₂, ZrB₂ and TiC particles for improved wear and corrosion resistance. *Surf. Coat. Technol.* **2019**, *364*, 323–329. [\[CrossRef\]](#)
17. Arulvel, S.; Elayaperumal, A.; Jagatheeshwaran, M.S.; Sathesh, K.A. Comparative Study on the Friction-Wear Property of As-Plated, Nd-YAG Laser Treated, and Heat-Treated Electroless Nickel-Phosphorus/ Crab Shell Particle Composite Coatings on Mild Steel. *Surf. Coat. Technol.* **2019**, *357*, 543–558. [\[CrossRef\]](#)
18. Delaunoy, F.; Vitry, V.; Bonin, L. (Eds.) *Electroless Nickel Plating Fundamentals to Applications*; CRC Press: Boca Raton, FL, USA, 2020.
19. Shi, L.; Sun, C.; Gao, P.; Zhou, F.; Liu, W. Mechanical properties and wear and corrosion resistance of electrodeposited Ni-Co/SiC nanocomposite coating. *Appl. Surf. Sci.* **2006**, *252*, 3591–3599. [\[CrossRef\]](#)
20. Jibo, J.; Haotian, C.; Lying, Z.; Qian, W.; Han, S.; Lin, H.; Huihui, W. Effect of heat treatment on structures and mechanical properties of electroless Ni-P-GO composite coatings. *RSC Adv.* **2016**, *6*, 10900.
21. Tamilarasan, T.R.; Sanjith, U.; Rajendran, R.; Rajagopal, G.; Sudagar, J. Effect of Reduced Graphene Oxide Reinforcement on the Wear Characteristics of Electroless Ni-P Coatings. *J. Mater. Eng. Perform.* **2018**, *27*, 3044–3053. [\[CrossRef\]](#)
22. Lee, C.K.; Teng, C.L.; Tan, A.H.; Yang, C.Y.; Lee, S.L. Electroless Ni-P/Diamond/Graphene Composite Coatings and Characterization of Their Wear and Corrosion Resistance in Sodium Chloride Solution. *Key Eng. Mater.* **2015**, *656*, 51–56. [\[CrossRef\]](#)

23. Sathir, M.H.; Saranya, M.; Aravind, M.; Srinivasan, A.; Siddharthan, A.; Rajendran, N. Comparison of in Situ and Ex Situ Reduced Graphene Oxide Reinforced Electroless Nickel Phosphorus Nanocomposite Coating. *Appl. Surf. Sci.* **2014**, *320*, 171–176. [[CrossRef](#)]
24. Jiang, N.; Fu, C.Q.; Wang, Z. Research on the Microstructure and Tribological Properties of the Electroless Ni–P-PTFE Composite Repairing Coating on Gears. *Appl. Mech. Mater.* **2013**, *327*, 136–139. [[CrossRef](#)]
25. Wu, H.; Liu, F.; Gong, W.; Ye, F.; Hao, L.; Jiang, J.; Han, S. Preparation of Ni–P–GO Composite Coatings and Its Mechanicals. *Surf. Coat. Technol.* **2015**, *272*, 25–32. [[CrossRef](#)]
26. Uysal, M. Electroless Codeposition of Ni–P Composite Coatings: Effects of Graphene and TiO₂ on the Morphology, Corrosion, and Tribological Properties. *Metall. Mater. Trans. A* **2019**, *50*, 2331–2341. [[CrossRef](#)]
27. Kumari, S.; Panigrahi, A.; Singh, S.K.; Pradhan, S.K. Corrosion-Resistant Hydrophobic Nanostructured Ni-Reduced Graphene Oxide Composite Coating with Improved Mechanical Properties. *J. Mater. Eng. Perform.* **2018**, *27*, 5889–5897. [[CrossRef](#)]
28. Hu, Q.-H.; Wang, X.-T.; Chen, H.; Wang, Z.-F. Synthesis of Ni/Graphene Sheets by an Electroless Ni-plating Method. *New Carbon Mater.* **2012**, *27*, 35–41. [[CrossRef](#)]
29. Yu, Q.; Zhou t Jiang, Y.; Yan, X.; An, Z.; Wang, X.; Zhang, D.; Ono, T. Preparation of Graphene-Enhanced Nickel-Phosphorus Composite Films by Ultrasonic-Assisted Electroless Plating. *Applied Surf. Sci.* **2018**, *435*, 617–625. [[CrossRef](#)]
30. Srivatswa, A.; Sarkar, S.; De, J.; Majumdar, G. Parametric optimization of electroless Ni-P-CNT coating using genetic algorithm to maximie the rate of deposition. *Mater. Today Proc.* **2022**, *66*, 3769–3774.
31. Rashad, M.; Pan, F.; Tang, A.; Asif, M. Effect of Graphene Nanoplatelets addition on mechanical properties of pure aluminum using a semi-powder method. *Prog. Nat. Sci. Mater. Int.* **2014**, *24*, 101–108. [[CrossRef](#)]
32. Mindivan, F.; Aydın, K.; Mindivan, H. Production and Characterization of Electrodeposited Nickel/Graphene Composite Coatings. *Nevşehir Bilim Ve Teknol. Derg.* **2019**, *8*, 29–36. [[CrossRef](#)]
33. Gao, X.; Yue, H.; Guo, E. Mechanical properties and thermal conductivity of graphene reinforced copper matrix composites. *Powder Technol.* **2016**, *301*, 601. [[CrossRef](#)]
34. Bardes, B.P. *Metals Handbook, Volume 3 Properties and Selection: Stainless Steels, Tool Materials and Species-Purpose Metals Titanium and Titanium Alloys*, 9th ed.; ASM: Almere, The Netherlands, 1980.
35. Tanrıöver, K.; Taşçı, A. Titanyum Alaşımlarının Isıl İşlemi. *Makine Mag.* **1997**, *1*, 58.
36. Brunette, D.M.; Tengwall, B.; Textor, M.; Thomsen, P. *Titanium in Medicine*; Springer: Heidelberg, Germany, 2001.
37. Long, M.; Rack, H.J. Titanium alloys in total joint replacement- a materials science perspective. *Biomaterials* **1998**, *19*, 1621–1639. [[CrossRef](#)]
38. Gupta, M.K.; Etri, H.E.; Korkmaz, M.E.; Ross, N.S.; Krolczyk, G.M.; Gawlik, J.; Pimenov, D.Y. Tribological and surface morphological characteristics of titanium alloys: A review. *Arch. Civ. Mech. Eng.* **2022**, *22*, 72. [[CrossRef](#)]
39. Shum, P.W.; Zhou, Z.F.; Li, K.Y. Investigation of the tribological properties of the different textured DLC coatings under reciprocating lubricated conditions. *Tribol. Int.* **2013**, *65*, 259–264. [[CrossRef](#)]
40. Kaur, S.; Ghadirinejad, K.; Reza, H.O. An Overview on the Tribological Performance of Titanium Alloys with Surface Modifications for Biomedical Applications. *Lubricants* **2019**, *7*, 65. [[CrossRef](#)]
41. Yılbaş, B.S.; Şahin, A.Z.; Al-Garni, A.Z.; Said, S.A.; Ahmed, Z.; Abdulaleem, B.J.; Sami, M. Plasma nitriding of Ti 6Al 4V alloy to improve some tribological properties. *Surf. Coat. Technol.* **1996**, *80*, 287–292. [[CrossRef](#)]
42. Schlesinger, M. *Modern Electroplating*, 5th ed.; John Wiley & Sons Inc: Toronto, ON, Canada, 2010.
43. Riedel, W. *Electroless Nickel Plating, Metals Park*; ASM International: Novelty, OH, USA, 1991.
44. Çakır, A.F. Akımsız Nikel Kaplamalar ve Uygulamaları. *Yüzey İşlemler* **2001**, *98*, 76–83.
45. Shahin, G.E. Comparison of Electroless Nickel & Functional Chromium. In Proceedings of the SUR/FIN 2009 Technical Conference, Louisville, KY, USA, 16–17 June 2009.
46. Meshram, A.P.; Kumar, M.K.P.; Srivastava, C. Enhancement in the corrosion resistance behaviour of amorphous Ni-P coatings by incorporation of graphene. *Diam. Relat. Mater.* **2020**, *105*, 107795. [[CrossRef](#)]
47. Yasin, G.; Khan, M.A.; Arif, M.; Shakeel, M.; Hassan, T.M.; Khan, W.Q.; Korai, R.M.; Abbas, Z.; Zuo, Y. Synthesis of spheres-like Ni/graphene nanocomposite as an efficient anti-corrosive coating; effect of graphene content on its morphology and mechanical properties. *J. Alloys Compd.* **2018**, *755*, 79–88. [[CrossRef](#)]
48. Brunelli, K.; Dabala, M.; Magrini, M. Diffusion treatment of Ni–B coatings by induction heating to harden the surface of Ti–6Al–4V alloy. *Mater. Chem. Phys.* **2009**, *115*, 467–472. [[CrossRef](#)]
49. Balaraju, J.N.; Saroary, J.; Anjana, J.; Rajam, K.S. Structure and phase transformation behavior of electroless Ni–P alloys containing tin and tungsten. *J. Alloys Compd.* **2007**, *436*, 319–327. [[CrossRef](#)]
50. Thomas, E.W.; Schlesinger, M. The Effect of Solution PH and Heat-Treatment on the Properties of Electroless Nickel-boron Films. *J. Electrochem. Soc.* **1994**, *141*, 78–82. [[CrossRef](#)]
51. Du, S.; Li, Z.; He, Z.; Ding, H.; Wang, X.; Zhang, Y. Effect of Temperature on the Friction and Wear Behavior of Electroless Ni–P–MoS₂–CaF₂ Self-Lubricating Composite Coatings. *Tribol. Int.* **2018**, *128*, 197–203. [[CrossRef](#)]
52. Wu, Y.T.; Lei, L.; Shen, B.; Hu, W.B. Investigation in Electroless NiP- Cg(Graphite)-SiC Composite Coating. *Surf. Coat. Technol.* **2006**, *201*, 441–445. [[CrossRef](#)]
53. Apachitei, I.; Duszczuk, J.; Katgerman, L.; Overkamp, P.J.B. Electroless Ni–P Composite Coatings: The Effect of Heat Treatment on The Microhardness of Substrate and Coating. *Scr. Mater.* **1998**, *38*, 1347–1353. [[CrossRef](#)]

54. Zhecheva, A.; Sha, W.; Malinov, S.; Long, A. Enhancing the microstructure and properties of titanium alloys through nitriding and other surface engineering methods. *Surf. Coat. Technol.* **2015**, *200*, 2192–2207. [[CrossRef](#)]
55. Praveen, B.M.; Venkatesha, T.V. Electrodeposition and properties of Zn–Ni–CNT composite coatings. *J. Alloys Compd.* **2009**, *482*, 53–57. [[CrossRef](#)]
56. Baudrand, D.W. *Electroless Nickel Plating*; ASM International: Materials Park, OH, USA, 1994.
57. Kumar, C.M.P.; Venkatesha, T.V.; Shabadi, R. Preparation and corrosion behavior of Ni and Ni–graphene composite coatings. *Mater. Res. Bull.* **2013**, *48*, 1477–1483. [[CrossRef](#)]
58. Algul, H.; Tokur, M.; Ozcan, S.; Uysal, M.; Cetinkaya, T.; Akbulut, H.; Alp, A. The effect of graphene content and sliding speed on the wear mechanism of nickel–graphene nanocomposites. *Appl. Surf. Sci.* **2015**, *359*, 340–348. [[CrossRef](#)]
59. Xu, Z.Q.; Zhang, X.; Shi, W.; Zhai, K.Y. Tribological Properties of TiAl Matrix Self-Lubricating Composites Containing Multilayer Graphene and Ti₃SiC₂ at High Temperatures. *Tribol. Trans.* **2015**, *58*, 1131–1141. [[CrossRef](#)]
60. Karşlıoğlu, R. Karbon Nanotüp Takviyeli Nikel-Kobalt Kaplamaların Geliştirilmesi. Ph.D. Thesis, Sakarya University, Serdivan, Turkey, 2014.
61. Karşlıoğlu, R.; Akbulut, H. Comparison microstructure and sliding wear properties of nickel–cobalt/CNT composite coatings by DC, PC and PRC current electrodeposition. *Appl. Surf. Sci.* **2015**, *353*, 615–627. [[CrossRef](#)]
62. Sharma, S.; Sangal, S.; Monda, K. On the optical microscopic method for the determination of ball-on-flat surface linearly reciprocating sliding wear volume. *Wear* **2013**, *300*, 82–89. [[CrossRef](#)]
63. Bai, H.; Zhong, L.; Kang, L.; Zhuang, W.; Lv, Z.; Xu, Y. A review on wear-resistant coating with high hardness and high toughness on the surface of titanium alloy. *J. Alloys Compd.* **2021**, *882*, 160645. [[CrossRef](#)]
64. Uygunoğlu, T.; Brostow, W.; Gunes, I. Wear and friction of composites of an epoxy with boron containing wastes. *Polimeros* **2015**, *25*, 271–276. [[CrossRef](#)]
65. Khrushchov, M. Resistance of metal to wear by abrasion as related to hardness. In Proceedings of the Conference Lubrication and Wear, London, UK, 1–3 October 1957; Institution of Mechanical Engineers: London, UK; pp. 655–659.
66. Tiwari, S.K.; Kumar, V.; Huczko, A.; Oraon, R.; Adhikari, A.D.; Nayak, G.C. Magical Allotropes of Carbon: Prospects and Applications. *Crit. Rev. Solid State Mater. Sci.* **2016**, *41*, 257–317. [[CrossRef](#)]
67. Zeng, Q.; Erdemir, A.; Eryılmaz, O. Ultralow Friction of ZrO₂ Ball Sliding against DLC Films under Various Environments. *Appl. Sci.* **2017**, *7*, 938. [[CrossRef](#)]
68. Penkov, O.V. *Tribology of Graphene: Simulation Methods, Preparation Methods, and Their Applications*; Elsevier Inc.: Zhejiang, China, 2020.
69. Zhang, W.; Li, Y.; Zeng, X.; Peng, S. Synergetic effect of metal nickel and graphene as a cocatalyst for enhanced photocatalytic hydrogen evolution via dye sensitization. *Sci. Rep.* **2015**, *5*, 10589. [[CrossRef](#)]
70. Johra, F.T.; Lee, J.W.; Jung, W.G. Facile and Safe Graphene Preparation on Solution-based platform. *J. Ind. Eng. Chem.* **2014**, *20*, 2883–2887. [[CrossRef](#)]
71. Binding Energy of Graphene (n.d). Available online: <https://www.jp.xpssimplified.com/elements/carbon.php> (accessed on 25 February 2022).
72. Malard, L.M.; Pimenta, M.A.; Dresselhaus, G.; Dresselhaus, M.S. Raman spectroscopy in graphene. *Phys. Rep.* **2009**, *473*, 51–87. [[CrossRef](#)]
73. Ferrari, A.C. Raman spectroscopy of graphene and graphite: Disorder, electron-phonon coupling, doping and nonadiabatic effects. *Solid State Commun.* **2007**, *143*, 47–57. [[CrossRef](#)]
74. Vidano, R.P.; Fischbach, D.B.; Willis, L.J.; Loehr, T.M. Observation of Raman Band Shifting with Excitation Wavelength for Carbons and Graphites. *Solid State Commun.* **1981**, *39*, 341–344. [[CrossRef](#)]